On the Spatiospectral Localization Optimality of the Discrete Hirschman Transform and Construction of Real-Valued 2D Separable Block Transforms

Elnaz Aghdaei[1], Obada Muhammad[2], Tomasz Przebinda[3], Murad Özaydın[3], and Joseph P. Havlicek[1]

***Abstract*—The discrete Hirschman transform provides a representation for discrete and finitely supported signals in terms of basis signals having optimal joint time-frequency localization with respect to an entropy-based discrete Hirschman uncertainty principle. This is significant in view of the fact that extending the traditional Heisenberg-Weyl inequality energy-based notion of uncertainty to the discrete and finitely supported case is problematic for several reasons. However, treatment of the discrete Hirschman transform has often been steeped in language and concepts from modern algebra that may be largely inaccessible to some engineering students and practicing engineers. In this paper, we first review the discrete Hirschman transform in the typical general setting. We then show how the construction of practical transforms can be presented using only concepts that should be accessible to engineering students after a basic course in DSP or image processing. We also explain the notion of joint localization as it applies to both discrete Hirschman transforms in general and the Hirschman optimal transform (HOT) in particular. Finally, we present a new algorithm for constructing real-valued 2D separable discrete Hirschman block transforms of arbitrary even square sizes.**

***Index Terms*—uncertainty principles, Hirschman transform, time-frequency localization, engineering education**

I. Introduction

As is well known, the uncertainty principle limits the degree to which a function $x \in L^2(\mathbb{R})$ with Fourier transform $X = \mathcal{F}x$ can be simultaneously localized in time and frequency by placing a lower bound on the time-bandwidth product according to

$$\sigma_t \sigma_f \geq \frac{1}{4\pi}, \tag{1}$$

where σ_t^2 and σ_f^2 are, respectively, the variance or "spread" of the signal $x(t)$ in time and in frequency. These variances may be rigorously interpreted as moments with respect to the distribution of the signal's energy in time and frequency. Gabor argued for representing general signals in terms of jointly well localized elementary signals and showed that the lower bound in (1) is uniquely achieved by the class of modulated and translated Gaussian pulses today known as *Gabor functions* [1]. These results were extended to $L^2(\mathbb{R}^2)$ by Daugman, who showed that the 2D Gabor functions achieve the lower bound in 2D.

This energy-based notion of uncertainty is presented in many textbooks, sometimes more qualitatively as the closely related concept of "reciprocal spreading." However, due at least in part to the difficulties inherent in defining a translation invariant discrete analogue of the continuous-domain variances σ_t^2, σ_f^2, direct extension of the energy-based principle (1) to a finitely supported discrete-time signal $x \in \ell^2(\mathbb{Z}/N\mathbb{Z})$ —i.e., precisely the type that are typically most important in practical DSP and image processing applications—is problematic. Yet we are not aware of any "standard" engineering textbooks that broach the topic of uncertainty measures for the $\ell^2(\mathbb{Z}/N\mathbb{Z})$ case, nor even the $\ell^2(\mathbb{Z})$ case, aside from a brief marginal note in [2, Sec. 7.4].[1]

There are at least two main viable options for extending the continuous-domain uncertainty principle (1) to the discrete and finitely supported case, including approaches based on the counting measure of the support of x and X [4] and those based on the entropy of x and X [5]. Here, we focus on the second option with an approach that leads to optimizers which define the discrete Hirschman transform [6], [7] and are decidedly not Gabor-like [8].

Our objectives in this paper are fourfold: (1) to clarify the spatiospectral localization optimality of the discrete Hirschman transform in a way that should be accessible to practicing engineers and engineering students, including clarifying a point that was not stated entirely clearly in [9]; (2) to clarify the distinction between discrete Hirschman transforms and the Hirschman optimal transform (HOT), again using accessible language; (3) to demonstrate construction of discrete Hirschman transforms in a way that can be presented to upper division undergraduate and graduate engineering students who often lack a foundation in modern algebra; and (4) to present a new algorithm for constructing real-valued 2D separable block Hirschman transforms for square blocks of arbitrary even sizes.

II. Background

In this section we briefly review the main theorem from [6], which provides a lower bound on discrete Hirschman uncertainty and identifies the minimizers. Let $A = \mathbb{Z}/N\mathbb{Z}$ be the ring $\{0, 1, 2, \ldots, N-1\}$ with addition and multiplication modulo N, let j be the imaginary unit, and let $W_N = \exp(-j2\pi/N)$. Let $x \in \ell^2(A)$ be a finite-length unit-norm discrete time-signal ($x : A \to \mathbb{C}$, $||x||_{\ell^2} = 1$). We formulate the DFT as a unitary transform (with the constant distributed symmetrically in both domains) according to

$$X[k] = (\mathcal{F}x)[k] = \frac{1}{\sqrt{N}} \sum_{n=0}^{N-1} x[n] W_N^{nk}, \tag{2}$$

$$x[n] = \frac{1}{\sqrt{N}} \sum_{k=0}^{N-1} X[k] W_N^{-nk}. \tag{3}$$

As in [5]–[8], [10], the localization of x is quantified by the entropy

$$H(x) = -\sum_{n=0}^{N-1} |x[n]|^2 \ln\left(|x[n]|^2\right). \tag{4}$$

The joint time-frequency localization of x may then be rigorously quantified by the measure

$$H_p(x) = pH(x) + (1-p)H(X), \tag{5}$$

where parameter $0 \leq p \leq 1$ balances the relative contributions of time and frequency localization to the joint spatiospectral measure H_p. In the special case $p = 1/2$ where the time and frequency

[1]E. Aghdaei and J.P. Havlicek are with the University of Oklahoma, School of Electrical & Computer Engineering, Norman, OK, USA.

[2]O. Muhammad is with the University of Oklahoma, Stephenson School of Biomedical Engineering, Norman, OK, USA.

[3]T. Przebinda and M. Özaydın are with the University of Oklahoma, Department of Mathematics, Norman, OK, USA.

[1]Although the subject does receive treatment in the more advanced reference [3] which may be appropriate for some advanced students.

contributions are weighted equally, the measure $H_{1/2}$ has been referred to as discrete or digital *Hirschman uncertainty*.

We can now state the main theorem from [6]. As a technical matter, the theorem considers that $x \in \ell^2(A)$ and $y \in \ell^2(A)$ with $||x||_{\ell^2} = ||y||_{\ell^2} = 1$ are equivalent if $\exists \lambda \in \mathbb{C}$ with $|\lambda| = 1$ such that $y = \lambda x$; in other words, if x and y are "the same" up to multiplication by a unit-magnitude complex constant. The theorem is then stated in terms of the set of these equivalence classes, which is denoted $P(A)$. The reason for this is that multiplication by such λ does not change H_p. Intuitively, this may be thought of as meaning that any member of an equivalence class in $P(A)$ can substitute for any other member of the same class. Note that membership in $P(A)$ implies $||x||_{\ell^2} = 1$.

Theorem (Main): Let $x \in P(A)$. Let B be a subgroup of A and let $|\cdot|$ denote cardinality. Let $\mathbb{I}_B[n]$ denote the indicator function of B. Then:

a) $H_{1/2}(x) \geq \frac{1}{2}\ln(|A|)$;
b) the set of vectors $x \in P(A)$ with $H_{1/2}(x) = \frac{1}{2}\ln(|A|)$ coincides with the union of the orbits

$$\rho(G_1(A))\frac{1}{\sqrt{|B|}}\mathbb{I}_B[B] \rightarrow W_N^{-(bn+c)}\frac{1}{\sqrt{|B|}}\mathbb{I}_B[n+a], \quad (6)$$

where $a, b, c, n \in A$, $G_1(A)$ is the Heisenberg group of degree one, and $G_1(A)$ is identified with $A \times A \times A$ through the map

$$G_1(A) \ni \begin{bmatrix} 1 & a & c \\ 0 & 1 & b \\ 0 & 0 & 1 \end{bmatrix} \rightarrow (a, b, c) \in A \times A \times A; \quad (7)$$

c) each orbit (6) is an orthonormal basis of $\ell^2(A)$;
d) the set of vectors $x \in P(A)$ such that $H_p(x) = \frac{1}{2}\ln(|A|)\ \forall\ 0 \leq p \leq 1$ is nonempty if and only if $|A|$ is a square, in which case it coincides with the orbit (6) for the unique subgroup $B \subseteq A$ of cardinality $|B| = \sqrt{|A|}$. ■

Part a) has been referred to in [5] and elsewhere as *the discrete Hirschman uncertainty principle*; it provides a lower bound on the joint spatiospectral localization of x with respect to $H_{1/2}$. Part b) identifies the signals $x \in \ell^2(A)$ that achieve the lower bound. Part c) guarantees that the minimizers from part b) are orthonormal bases for $\ell^2(A)$ (and can be used to construct corresponding unitary transforms). Finally, part d) states that when N is a square there is a unique subgroup B that is optimal in the sense that the signals x in the orthonormal basis it generates achieve the lower bound $\frac{1}{2}\ln(|A|)$ on joint localization for $p = 1/2$ and, moreover, maintain this same value for $H_p(x)$ across *all* $0 \leq p \leq 1$, i.e., irrespective of the relative weighting of time and frequency. We will discuss this in more detail in Sections IV and VI.

III. Discrete Hirschman Transform

In this section, we will use language and concepts that should be accessible to upper division undergraduate and beginning graduate level engineering students to show how the main theorem of Section II can be applied to construct discrete Hirschman transforms applicable to finite-length discrete-time signals. Suppose we have N-point discrete time signals $x[n]$ defined for $0 \leq n \leq N-1$. Then $A = \{0, 1, 2, \ldots, N-1\}$.

The first thing we need is to select a subgroup B of A along with its indicator function $\mathbb{I}_B$. The number of subgroups available is equal to the number of positive factors of N. There are three straightforward ways to obtain the candidate subgroups and indicator functions.

1) We can generate the subgroups directly. Even though our target audience may be lacking any background in modern algebra, this can be explained as a process of, for each positive factor of N, taking the union of the integer multiples modulo N until only repeated values are obtained. For example, if $N = 6$, then $A = \{0, 1, 2, 3, 4, 5\}$ and the positive factors of N are 1, 2, 3, and 6. Noting that $6 \bmod 6 = 0$, we obtain the subgroups

$$\begin{aligned} \langle 0\rangle = \{0\} &\mapsto \mathbb{I}_B[n] = [1\ 0\ 0\ 0\ 0\ 0] \\ \langle 1\rangle = \{0\ 1\ 2\ 3\ 4\ 5\} &\mapsto \mathbb{I}_B[n] = [1\ 1\ 1\ 1\ 1\ 1] \\ \langle 2\rangle = \{0\ 2\ 4\} &\mapsto \mathbb{I}_B[n] = [1\ 0\ 1\ 0\ 1\ 0] \\ \langle 3\rangle = \{0\ 3\} &\mapsto \mathbb{I}_B[n] = [1\ 0\ 0\ 1\ 0\ 0]. \end{aligned}$$

2) Alternatively, the subgroup generation process can be presented as one of applying periodization to the Kronecker delta

$$\delta[n] = \begin{cases} 1 & n = 0, \\ 0 & \text{otherwise}, \end{cases} \quad (8)$$

as described in [8].[2]

Definition: for $N = KL$, the periodization of $v \in \mathbb{C}^K$ is $x \in \mathbb{C}^N$ given by $x(sK + r) = v[r]$ for $0 \leq s \leq L-1$ and $0 \leq r \leq K-1$.

For example, if $N = 6$, we obtain

$$\begin{aligned} &\{K, L\} = \{6, 1\}\colon v[n] = [1\ 0\ 0\ 0\ 0\ 0] \mapsto \mathbb{I}_B[n] = [1\ 0\ 0\ 0\ 0\ 0] \\ &\{K, L\} = \{1, 6\}\colon v[n] = [1] \mapsto \mathbb{I}_B[n] = [1\ 1\ 1\ 1\ 1\ 1] \\ &\{K, L\} = \{2, 3\}\colon v[n] = [1\ 0] \mapsto \mathbb{I}_B[n] = [1\ 0\ 1\ 0\ 1\ 0] \\ &\{K, L\} = \{3, 2\}\colon v[n] = [1\ 0\ 0] \mapsto \mathbb{I}_B[n] = [1\ 0\ 0\ 1\ 0\ 0] \end{aligned}$$

3) As a third alternative, the subgroup generation process can be described as one of starting with $\mathbb{I}_B[n] = 1$, $0 \leq n \leq N-1$, then applying upsampling by the factors $K > 1$ given in the second alternative above, and finally retaining the result for $0 \leq n \leq N-1$ only. This yields exactly the same subgroups and indicator functions as the first two options.

A 1D discrete Hirschman transform can then be constructed from each subgroup by using the subgroup indicator function to generate an orthonormal basis for $\ell^2(A)$ and then setting the rows of the transform matrix equal to the basis vectors (in any order). As indicated by parts b) and c) of the main theorem in Section II and equivalently in terms of operations on discrete-time signals by Theorem 2 of [8], the first basis vector is then

$$e_1[n] = \frac{1}{\sqrt{|B|}}\mathbb{I}_B[n]. \quad (9)$$

Additional unit-norm basis vectors may then be generated by applying arbitrary compositions of the following operations to $e_1[n]$ until N orthonormal basis vectors are obtained:

1) translation modulo N: $T_a v[n] = v[(n-a) \mod N]$,
2) modulation: $M_b v[n] = W_N^{-bn} v[n]$,
3) length-N DFT.

Each of these basis vectors will admit optimal spatiospectral localization in the sense of achieving the lower bound $\frac{1}{2}\ln N$ on $H_{1/2}$.

As an illustrative example to conclude this section, suppose that $N = 6$ and we choose the subgroup $B = \langle 2\rangle = \{0\ 2\ 4\}$. Then according to (9) the first basis vector is given by

$$e_1[n] = \frac{1}{\sqrt{3}}[1\ 0\ 1\ 0\ 1\ 0]. \quad (10)$$

[2]There is an additional scale factor of $1/\sqrt{L}$ in the definition given in [8] that is not needed here because it is already included explicitly in part b) of the main theorem as the factor $1/\sqrt{|B|}$.

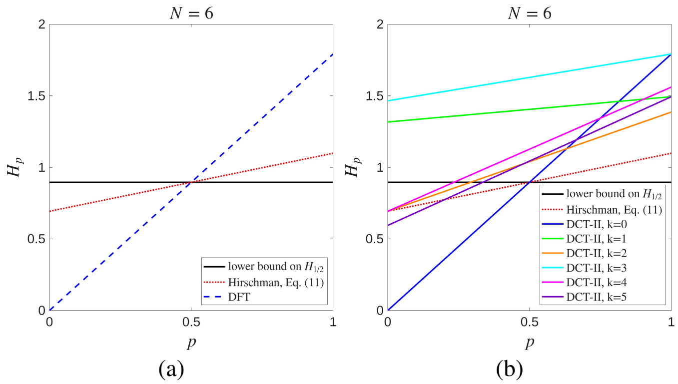

Fig. 1. Joint localization measure H_p versus p for some length-6 transforms. The lower bound on $H_{1/2}$ is shown in black. (a) discrete Hirschman (11) and DFT – for these two, the graph is the same for all six basis signals; (b) discrete Hirschman transform (11) and six basis signals of the Type-II DCT.

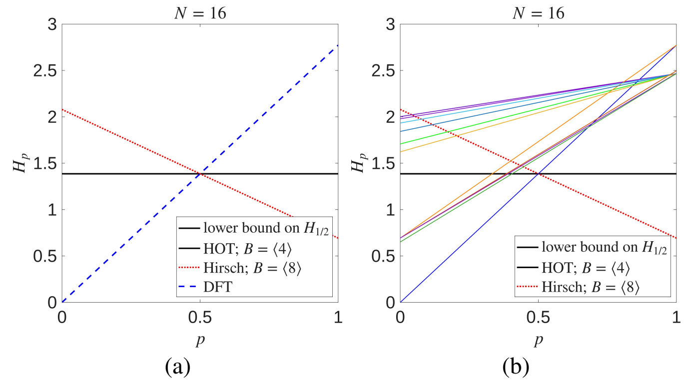

Fig. 2. Joint localization measure H_p versus p for several 16-point transforms. The lower bound on $H_{1/2}$ is shown in black. (a) HOT (equal to the lower bound on $H_{1/2}$ $\forall$ p), discrete Hirschman with $B = \langle 8 \rangle$, and DFT; (b) HOT, discrete Hirschman with $B = \langle 8 \rangle$, and basis signals of the Type-II DCT.

Next, we let $e_2[n] = T_1 e_1[n]$, $e_3[n] = M_5 e_1[n]$, $e_4[n] = T_1 e_3[n]$, $e_5[n] = M_4 e_1[n]$, and $e_6[n] = T_1 e_5[n]$ to obtain the discrete Hirschman transform matrix (note: $W_6^8 = W_6^2$)[3]

$$\mathcal{H}_6 = \frac{1}{\sqrt{3}} \begin{bmatrix} 1 & 0 & 1 & 0 & 1 & 0 \\ 0 & 1 & 0 & 1 & 0 & 1 \\ 1 & 0 & W_6^2 & 0 & W_6^4 & 0 \\ 0 & 1 & 0 & W_6^2 & 0 & W_6^4 \\ 1 & 0 & W_6^4 & 0 & W_6^8 & 0 \\ 0 & 1 & 0 & W_6^4 & 0 & W_6^8 \end{bmatrix}. \tag{11}$$

IV. Hirschman Optimal Transform (HOT)

When N is a square, it becomes possible to construct a special discrete Hirschman transform called the *Hirschman optimal transform* or HOT. Eq. (5) shows that $H_p(x)$ is linear in p with a slope of $H(x) - H(X)$. Plots of H_p as a function of p for the length-6 discrete Hirschman transform (11), the 6-point DFT, and the 6-point type-II DCT are shown in Fig. 1. For each of $\mathcal{H}_6$ in (11) and the DFT (2), all six basis signals yield the same plot; these two distinct plots are shown in Fig. 1(a) where it may be seen that both achieve the lower bound on joint localization at $p = 1/2$. This is because the DFT *is* a Hirschman transform deriving from the subgroup $\langle 0 \rangle$ with periodization $\{K, L\} = \{1, N\}$. For the DCT, the p-H_p characteristic exhibits generally different slopes and intercepts for each basis signal as shown in Fig. 1(b) where the $\mathcal{H}_6$ transform (11) is also shown. One thing evident from Fig. 1 is that any unitary transform which achieves a high degree of joint localization manifest as small $H_p \ll (1/2)\ln N$ for some p must necessarily exhibit correspondingly poor joint localization $H_p \gg (1/2)\ln N$ for some other set of p. Moreover, part a) of the main theorem mandates that every curve must be at or above $(1/2)\ln N$ at $p = 1/2$, which may be thought of as a minimum "fulcrum point" of the p-H_p curve.

The Hirschman optimal transform optimizes the joint spatiospectral localization measure H_p simultaneously *for all* p in the following sense: the p-H_p characteristic passes through the theoretically optimal fulcrum point $(1/2)\ln N$ at $p = 1/2$ and has a slope of zero, remaining fixed at that $H_{1/2}$-optimal value for *all* p. Thus, it follows from part d) of the main theorem and linearity of the p-H_p characteristic that any other unitary transform which delivers *better* joint localization than the HOT at some p on one side of the fulcrum point $p = 1/2$ must necessarily deliver correspondingly *worse* joint localization than the HOT for all p in the half-line on the other side of the fulcrum point. Moreover, part d) of the main theorem guarantees that the HOT is the *only* unitary transform which can provide a p-H_p characteristic that passes through the optimal fulcrum point at $p = 1/2$ with a slope of zero; any other unitary transform must perform worse (in terms of joint localization) at least on a half-line to one side or the other of the $p = 1/2$ fulcrum point.

Note that no HOT exists for $N = 6$, which is the case that we have up to now been using as an illustrative example. This is because the HOT exists if and only if N is a square – and it is unique (for any given value of N and up to equivalence classes $P(A)$) when it does exist, deriving from the unique subgroup of cardinality $\sqrt{N}$ and corresponding to the periodization $\{K, L\} = \{\sqrt{N}, \sqrt{N}\}$. Examples showing construction of the 9-point HOT were given in [6], [11], including Matlab code for implementing the K^2-point HOT for arbitrary $K \in \mathbb{Z}^+$. To further clarify the distinction between the HOT and the general discrete Hirschman transform, as well as the sense in which the HOT admits optimal joint spatiospectral localization, graphs of H_p versus p for the case of $N = 16$ are given in Fig. 2 for several transforms. In both Fig. 2(a) and (b), the black horizontal line is the theoretical lower bound on $H_{1/2}$ which coincides with the p-H_p characteristic of the 16-point HOT for $B = \langle 4 \rangle$, $\{L, K\} = \{4, 4\}$, and $v[n] = [1\ 0\ 0\ 0]$. In both parts of Fig. 2, the red dashed line gives the p-H_p characteristic for the discrete Hirschman transform with $B = \langle 8 \rangle$, $\{L, K\} = \{8, 2\}$, and $v[n] = [1\ 0\ 0\ 0\ 0\ 0\ 0\ 0]$, which is not a HOT. The other curves in Fig. 2(b) are for the basis signals of the 16-point Type-II DCT.

For the DFT (2) we have basis signals $e_m[n]$ with $(\mathcal{F}e_m)[k] = \delta[k - m]$ and so, for $p = 0$ in (5), we obtain $H_0(e_m) = 0$ as shown in Fig. 2(a). According to part b) of the main theorem, there is also a dual discrete Hirschman transform with basis signals $e_m[n] = \delta[n - m]$ that yields $H_1(e_m) = 0$ for $p = 1$. Thus it is clear that, for unit-norm discrete-time signals $x[n]$ defined for $0 \le n \le N - 1$, H_p is bounded according to $H_0 \ge 0$, $H_{1/2} \ge (1/2)\ln N$, and $H_1 \ge 0$. Bounds on H_p for other p are not yet known at this time. However, the p-H_p characteristic must be linear in p and only a HOT can both achieve the minimal value $(1/2)\ln N$ at $p = 1/2$ and provide a slope of zero. This implies that any other unitary transform must have worse joint localization relative to the HOT for $p < 1/2$, for $p > 1/2$, or both, and that is what is meant by statements that the HOT optimizes H_p simultaneously for all p: the HOT delivers $H_p = (1/2)\ln N$ $\forall$ p and any unitary transform that achieves a lower H_p for some particular p must have correspondingly worse joint localization at $1 - p$ in the sense that H_{1-p} must be correspondingly $> (1/2)\ln N$.

V. Separable 2D Block Hirschman Transform

Parts a), b), and c) of the main theorem in Section II have been generalized to the multidimensional finitely supported case in [13]. However, extension of part d) to the multidimensional case remains an open problem to the best of our knowledge. Therefore, we restrict our attention here to separable 2D transforms implemented by applying a 1D discrete Hirschman transform sequentially to the rows and columns of an image or image block.

[3]For easy and accessible explanation of why M_5 and M_4 are chosen for rows 3 and 5 of $\mathcal{H}_6$ in (11), note that $5 = -1 \bmod 6$, $4 = -2 \bmod 6$, and part b) of the main theorem requires $b \in A$ for the modulation operator M_b.

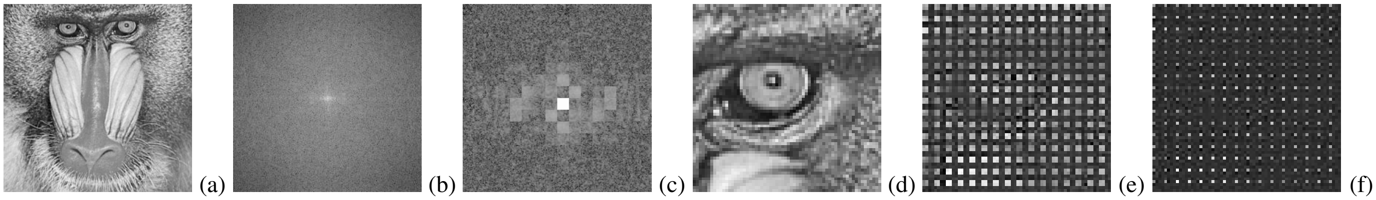

Fig. 3. Examples. (a) mandrill luma image; (b) centered FFT log-magnitude spectrum; (c) centered 2D separable HOT log-magnitude spectrum implemented in floating point but otherwise as described in [12]; (d) 64×64 ROI; (e) block 4×4 HOT (13) of (d); (f) block 4×4 2D DCT of (d).

Let $N = 4$, $B = \langle 2 \rangle = \{0\ 2\}$, and $\{K, L\} = \{2, 2\}$ to obtain $e_1[n] = (1/\sqrt{2})[1\ 0\ 1\ 0]$. Applying operators T_1, M_1, and $(T_1 \circ M_1)$ to $e_1[n]$ then yields an involutory transform matrix

$$\mathcal{H}_4 = \frac{1}{\sqrt{2}} \begin{bmatrix} 1 & 0 & 1 & 0 \\ 0 & 1 & 0 & 1 \\ 1 & 0 & -1 & 0 \\ 0 & 1 & 0 & -1 \end{bmatrix} \tag{12}$$

defining a 1D Hirschman optimal transform (HOT) on $\ell^2(\mathbb{Z}/4\mathbb{Z})$. The scaled matrix $\mathcal{B}_4 = \sqrt{2}\mathcal{H}_4$ may then be applied separably to the rows and columns of 4×4 image blocks $\mathbf{X}$ according to

$$\mathbf{Y} = \mathcal{H}_{4\times4}\{\mathbf{X}\} \equiv \mathcal{B}_4 \mathbf{X} \mathcal{B}_4, \tag{13}$$

$$\mathbf{X} = \mathcal{H}_{4\times4}^{-1}\{\mathbf{Y}\} \equiv (\mathcal{B}_4 \mathbf{Y} \mathcal{B}_4)/4 \tag{14}$$

to realize a separable 2D Hirschman optimal 4×4 block transform that is inherently real and integer-valued, requires only additions for the forward transform (13), and requires only additions and bit shift operations for the inverse transform (14).

This scheme can be extended to construct real and integer-valued separable 2D discrete Hirschman transforms applicable to square image blocks of arbitrary even sizes $N\times N$ using a 1D transform matrix

$$\mathcal{H}_N = \mathcal{H}_1 \otimes \mathbf{I}_{\frac{N}{2}\times\frac{N}{2}}, \tag{15}$$

where $\otimes$ is the Kronecker product, $\mathbf{I}_{\frac{N}{2}\times\frac{N}{2}}$ is the $\frac{N}{2}\times\frac{N}{2}$ identity matrix, and

$$\mathcal{H}_1 = \frac{1}{\sqrt{2}} \begin{bmatrix} 1 & 1 \\ 1 & -1 \end{bmatrix} \tag{16}$$

is the standard 2×2 Hadamard matrix. Note that in view of part d) of the main theorem, real integer transforms constructed using the new relation (15) are discrete Hirschman transforms but they are not Hirschman optimal transforms unless $N = 4$, in which case (15) coincides with the HOT matrix (12).

Examples are given in Fig. 3. The 256×256 *mandrill* image is shown in Fig. 3(a). Fig. 3(b) gives the FFT centered log-magnitude spectrum while the centered HOT log-magnitude spectrum $\mathbf{Y} = \mathcal{H}_{256}\mathbf{X}\mathcal{H}_{256}^T$ is given in Fig. 3(c). Fig. 3(d) shows a 64×64 region of interest (ROI) cropped from (a) to facilitate legible display of the 4×4 block transforms shown in (e), the real and integer separable 2D 4×4 block HOT (13), and (f), the block 4×4 2D DCT-II.

VI. Discussion and Conclusion

Discrete Hirschman transforms achieve optimal joint localization H_p in (5) for $p = 1/2$. For a given signal length N, the Hirschman optimal transform (HOT) exists if N is a square and uniquely provides optimal H_p joint localization simultaneously for all $0 \leq p \leq 1$ in the sense that the minimum value is achieved at $p = 1/2$ and maintained $\forall\ p$. Any unitary transform that achieves better joint localization for some $p < 1/2$ or $> 1/2$ must deliver correspondingly worse joint localization relative to the HOT $\forall\ p$ on the other side of the fulcrum point $p = 1/2$ as illustrated in Figs. 1 and 2. Demonstrated applications of 2D discrete Hirschman transforms and HOT include fast 2D convolution [14], including fast CNN convolution [15], 2D fractional HOT [16], and HOT domain color image enhancement [17]. Our main contributions in this paper were to clarify the notion of joint localization optimality and show how construction of Hirschman transforms can be presented in a way that is accessible to upper-division undergraduate and graduate students without using abstract algebra and to present a new algorithm for constructing real-valued integer 2D separable block Hirschman transforms for square blocks of arbitrary even sizes.

References

[1] D. Gabor, "Theory of communication," *J. Inst. Elect. Eng. London*, vol. 93, no. III, pp. 429–457, 1946.

[2] R. C. Gonzalez and R. E. Woods, *Digital Image Processing*, 4th ed. Pearson, 2017.

[3] H. Feichtinger and T. Strohmer, Eds., *Gabor Analysis and Algorithms: Theory and Applications*. Springer, 1998.

[4] D. Donoho and P. Stark, "Uncertainty principles and signal recovery," *SIAM J. Appl. Math.*, vol. 49, no. 3, pp. 906–931, Jun. 1989.

[5] A. Dembo, T. Cover, and J. Thomas, "information theoretic inequalities," *IEEE Trans. Inf. Theory*, vol. 37, no. 6, pp. 1501–1518, Nov. 1991.

[6] T. Przebinda, V. DeBrunner, and M. Özaydın, "The optimal transform for the discrete Hirschman uncertainty principle," *IEEE Trans. Inf. Theory*, vol. 47, no. 5, pp. 2086–2090, Jul. 2001.

[7] V. DeBrunner, M. Özaydın, T. Przebinda, and J. Havlicek, "The optimal solutions to the continuous- and discrete-time versions of the Hirschman uncertainty principle," in *Proc. IEEE Int'l. Conf. Acoust., Speech, Signal Process.*, Istanbul, Turkey, Jun. 5-9, 2000, pp. 81–84.

[8] V. DeBrunner, J. Havlicek, T. Przebinda, and M. Özaydın, "Entropy-based uncertainty measures for $L^2(\mathbb{R}^n)$, $\ell^2(\mathbb{Z})$, and $\ell^2(\mathbb{Z}/N\mathbb{Z})$ with a Hirschman optimal transform for $\ell^2(\mathbb{Z}/N\mathbb{Z})$," *IEEE Trans. Signal Process.*, vol. 53, no. 8, pp. 2690–2699, Aug. 2005.

[9] J. Havlicek, T. Arian, H. Soltani, T. Przebinda, and M. Özaydın, "A preliminary case for Hirschman transform video coding," in *Proc. IEEE Southwest Symp. Image Anal., Interp.*, Santa Fe, NM, Mar. 29-31 2020, pp. 104–107.

[10] V. DeBrunner, M. Özaydın, and T. Przebinda, "Analysis in a finite time-frequency plane," *IEEE Trans. Signal Process.*, vol. 48, no. 6, pp. 1831–1832, Jun. 2000.

[11] V. DeBrunner and E. Matusiak, "An algorithm to reduce the complexity required to convolve finite length sequences using the Hirschman optimal transform (HOT)," in *Proc. IEEE Int'l. Conf. Acoust., Speech, Signal Process.*, Hong Kong, Apr. 6-10, 2003, pp. II–577 – II–580.

[12] R. Thomas, V. DeBrunner, and L. DeBrunner, "Fixed-point implementation of discrete Hirschman transform," in *Proc. 52nd Asilomar Conf. Signals, Syst., Comput.*, Pacific Grove, CA, Oct. 28-31, 2018, pp. 1507–1511.

[13] M. Özaydın and T. Przebinda, "An entropy-based uncertainty principle for a locally compact abelian group," *J. Functional Anal.*, vol. 215, no. 1, pp. 241–252, 2004.

[14] W. Wang, L. DeBrunner, and V. DeBrunner, "An efficient hardware implementation of 2D convolution based on the discrete Hirschman transform," in *Proc. IEEE Int'l. Symp. Circuits, Syst.*, London, UK, May 25-28, 2025, 5 pp.

[15] W. Wang, V. DeBrunner, L. DeBrunner, D. Xue, H. Zhao, and R. Tao, "Very efficient convolutional neural network based on the discrete Hirschman transform," in *Proc. 58th Asilomar Conf. Signals, Syst., Comput.*, Pacific Grove, CA, Oct. 27-30, 2024, pp. 1344–1348.

[16] W.-L. Hsue, S.-C. Pei, and J.-J. Ding, "Efficient discrete fractional Hirschman optimal transform and its application," in *Proc. IEEE Int'l. Conf. Acoust., Speech, Signal Process.*, Prague, Czech Republic, May 22-27, 2011, pp. 3604–3607.

[17] B. Narsimha, E. Suresh, K. P. Chandar, and B. Komuraiah, "Enhancement of color images in HOT domain with quantitative measurements using entropy and relative entropy," in *Proc. Int'l. Conf. Signal, Image Process.*, Chennai, India, Dec. 15-17, 2010, pp. 34–38.